Journal of Radioanalytical and Nuclear Chemistry (2018) 316:673–683
https://doi.org/10.1007/s10967-018-5771-y

Sorption behavior of ^{85}Sr onto manganese oxides with tunnel structure

A. I. Ivanets[1] · V. G. Prozorovich[1] · T. F. Kouznetsova[1] · A. V. Radkevich[2] · P. V. Krivoshapkin[3] · E. F. Krivoshapkina[3] · M. Sillanpää[4,5]

Received: 15 January 2018 / Published online: 2 March 2018

Abstract

Sorption behavior of strontium ions on manganese oxides obtained by sol–gel technique reduction of $KMnO_4$ by different reagents (H_2O_2, $MnCl_2$ and polyvinyl alcohol) was studied. Sorption capacity of the most effective sorbent reaches 200 mg g^{-1} and distribution coefficient K_d (^{85}Sr)—3.67 × 10^5 cm^3 g^{-1}. Ion-exchange and chemisorption mechanism of strontium ions removal by manganese oxides were confirmed by means XRD, FT-IR, N_2 adsorption–desorption and SEM–EDX methods. The obtained sorbents are promising for liquid radioactive water treatment from strontium radionuclides.

Keywords Sorption · ^{85}Sr removal · Manganese oxides · Sol–gel synthesis · Sorption mechanism

Introduction

Radioactive waste contamination of the environment is one of the global ecological problems of our time. This is due to the operation of the nuclear power plants (NPP) and nuclear energy facilities, which leads to the formation of large amounts of liquid radioactive waste (LRW) that require processing and decontamination [1–3]. For example, operation of NPP based on the fast neutron reactor with electrical capacity of 600 MW results to annual discharges of radionuclides with waste water in volume 81 000 m^3, with a total activity about 3.9 × 10^{11} Bq [4]. One of the long-living radionuclides included in the LRW and which pose a significant threat to human and living organisms is the radionuclide ^{90}Sr [5, 6]. The half-life of ^{90}Sr isotope is 28.79 years. Chemical properties of Sr^{2+} are similar to Ca^{2+} ions, which complicates the task of purification of LRW and requires the development of materials for selective removal of Sr^{2+} ions from multicomponent aqueous solutions with high salinity.

Adsorption is the most effective and economically feasible method of purification of aqueous solutions containing trace amounts of Sr^{2+} [7–10]. In addition, this method allows selectively extract Sr^{2+} ions and its radionuclides from real polluted aquatic medium and LRW, thereby most effectively minimizing the amount of waste generated. In recent years, polymeric adsorbents functionalized with organic various acids have been used to control adsorption capacity and to provide selective adsorption of Sr^{2+} ions from aqueous solutions [11–13]. At the same time, inorganic sorption materials (zeolites, clays, metal oxides, etc.) have certain advantages over organic ion exchangers when using for treatment of liquid radioactive wastes due to their high chemical (pH range 0–14 and 2–12, respectively) and radiation stability (more than 10^8 Gray (Gy) and 10^5–10^6 Gy, respectively), compatibility with likely immobilization matrices such as cement and selectivity in relation to Sr^{2+} ions [14–17]. It is important to note that the selective properties are determined by the nature of the matrix of the

---

✉ A. I. Ivanets
ivanets@igic.bas-net.by

[1] Institute of General and Inorganic Chemistry of the National Academy of Sciences of Belarus, st. Surganova 9/1, 220072 Minsk, Belarus

[2] Joint Institute for Power and Nuclear Research – Sosny of the National Academy of Sciences of Belarus, PO Box 119, 220109 Minsk, Belarus

[3] ITMO University, Saint Petersburg, Russian Federation 197101

[4] Laboratory of Green Chemistry, Lappeenranta University of Technology, Sammonkatu 12, 50130 Mikkeli, Finland

[5] Department of Civil and Environmental Engineering, Florida International University, Miami 33174, USA

sorbent, state of radionuclides in the aquatic environment, nature and concentration of related compounds [18].

High exchange capacity, stability in alkaline media allow to consider manganese oxides with a layered and channel structure as a promising materials for the removal of radioactive metal ions from aqueous media [19]. Moreover, the performance of manganese oxides in comparison with inorganic sorbents (such as zirconium phosphate, titanium phosphate and titanium dioxide, which decreased at dose 2.19 MGy) and organic sorbents (efficiency is significantly reduced by doses of 0.1–1.0 MGy) is maintained up to the irradiation with dose 10 MGy [20]. Manganese oxides have a structure of octahedral molecular sieves (OMS) with tunnels 2 × 2 or 3 × 3, which is formed from octahedra MnO_6 [21, 22]. The dimensions of the tunnels of OMS-2 (cryptomelane with ions K^+) and OMS-1 (type todorokite with ions Ca^{2+} or Mg^{2+}) depend on the cations located inside and around of 0.46 and 0.70 nm respectively [23, 24].

According to the reference study of [25], in comparison with other types of organic and inorganic sorbents, manganese oxides are relatively highly selective towards Sr^{2+} ions in the presence of Na^+, Ca^{2+} and Mg^{2+} ions. At sorption from solutions, also containing 0.1 M $NaNO_3$ and 0.01 M $Ca(NO_3)_2$, K_d values for sorbent MDM [mixed manganese oxides (III, IV)] are $3.5–4.0 \times 10^4$ and $1.5–2.1 \times 10^3$ cm^3 g^{-1}, respectively. The authors [26] studied the sorption of the radionuclide ^{85}Sr and ^{137}Cs from aqueous solutions (in deionized H_2O) on synthetic manganese oxides with tunnel structure. For the oxides of cryptomelane type K_d^{Cs} and K_d^{Sr} are equal to 7.4×10^3 and $> 10^6$ cm^3 g^{-1}, and for oxides of the todorokite type values K_d^{Cs} and K_d^{Sr} are 5.0×10^4 and $> 10^6$ cm^3 g^{-1} respectively. In reference study of [27] the values of K_d for the materials of composition $K_{2x}Mn_xSn_{3-x}S_6$ ($x = 0.5–0.95$), or KMS-1 were determined. The value of K_d in distilled water is equal to 1.58×10^5 cm^3 g^{-1}. On the background of complex salt composition containing 3.70 Mg^{2+}, 11.14 Ca^{2+}, 9.17 Cs^+, 25.96 Na^+ and 4.60 mg dm^3 Sr^{2+} affinity of strontium is greater than for other cations mixture ($K_d = 1.83 \times 10^4$ cm^3 g^{-1}).

This work is devoted to study the mechanism of Sr^{2+} ions sorption from aqueous solutions onto tunnel manganese oxides obtained by the sol–gel method with the reducing $KMnO_4$ by different reagents—$MnCl_2$, H_2O_2, PVA. The relationship between the conditions of preparation, physical–chemical and sorption-selective properties of manganese oxides will allow to define general regularities and approaches to the directed synthesis of highly selective sorbents of strontium radionuclides.

Experimental

Manganese oxides synthesis

Sorbents based on manganese oxides were obtained with sol–gel method by reducing $KMnO_4$ in aqueous medium by PVA and inorganic reagents—H_2O_2 or $MnCl_2$ [28, 29]. To prepare the respective aqueous solutions used distilled water and reagents—$KMnO_4$, H_2O_2 (30 wt% aqueous solution), $MnCl_2·4H_2O$ and PVA (fully saponified, state standard 10779-78). All chemicals were of analytical grade and utilized as purchased from Five Oceans (Belarus) without further purification.

To 50 cm^3 of 0.1 wt% aqueous solution of $KMnO_4$, various amounts of 1.0 wt% aqueous solution H_2O_2 (2.2 cm^3) and 0.1 wt% aqueous solution $MnCl_2$ (0.4 cm^3) solutions were added dropwise with continuous stirring. Molar ratio of $KMnO_4$:H_2O_2 and $KMnO_4$:$MnCl_2$ equal to 1.00:1.25 and 1.0:1.5, respectively. As a result of getting a dark brown sol with a content of 0.05 wt% MnO_2, pH 10.8 and ζ-potential − 21.9 mV (H_2O_2—reducing agent). In the case of using $MnCl_2$ the content of MnO_2 in sol is 0.02 wt%, pH 4.4, ζ-potential − 17.5 mV. Hydrogels were obtained as a result of aging or electrolyte coagulation of sols which were subjected to heat treatment in a laboratory furnace SNOL 7,2/1300 in air at 400 °C for 3 h, the heating rate was 5 °C/min.

Using 0.5 wt% PVA like reducing agent, to 25 cm^3 of it, 25 cm^3 of $KMnO_4$ solution (0.5 wt%) was added in order to obtain 1.0:1.5 $KMnO_4$/$MnCl_2$ molar ratio.

In the third case, manganese oxide sol was prepared by adding dropwise 0.5 wt% aqueous solution of $KMnO_4$ under vigorous stirring to the 0.5 wt% aqueous PVA solution, the mass ratio of $KMnO_4$:PVA is 1:1. Thus formed colloidal solution is dark brown. The content of MnO_2 in sol is 0.33 wt%, pH 10.2, ζ-potential − 25.1 mV. The resulting hydrogel was washed with distilled water, dried in air at room temperature and calcined at 450 °C for 3 h, the heating rate was 5 °C min^{-1}.

Sorption study

Sorption properties of the synthesized sorbents towards Sr^{2+} ions were studied in static conditions at V/m ratio = 250 cm^3 g^{-1} (V—volume of the solution that contains the sorbed Sr^{2+} ions (10 cm^3); m—mass of the synthesized sorbents (0.04 g) with use of stable strontium ions and ^{85}Sr radionuclide at standard conditions (25 °C, 1 bar). In the first case, sorption of Sr^{2+} ions was carried out from $Sr(NO_3)_2$ solutions [analytical grade, Five Oceans (Belarus)] with concentration of Sr^{2+} 2000 mg dm^{-3} and pH 5.6. Concentration of Sr^{2+} in initial solution and after contact with sorbents (24 h) was defined on atomic absorbing spectrometer AAS Contr AA 300 (Germany). For solution containing radionuclide ^{85}Sr pH value was 5.59. The activity of initial solutions (A_0, kBq cm^3) and after sorption (A_e, kBq cm^3) was carried out on a gamma beta spectrometer of MKS AT1315 (Belarus). For studying of influence of sodium and calcium ions on strontium removal efficiency the aqueous solutions were prepared with addition of 0.1 M NaCl and 0.05 M $CaCl_2$.

Sorption capacity (Q, mg g^{-1}) and distribution coefficient (K_d, cm^3 g^{-1}) of ^{85}Sr radionuclide were calculated by the following equations:

$$Q = \frac{(C_0 - C_e) \times V}{m} \tag{1}$$

$$K_d = \frac{A_0 - A_e}{A_e} \times \frac{V}{m} \tag{2}$$

where C_0 and C_e—initial and equilibrium concentration of Sr^{2+} ions, mg g^{-1}, respectively, A_0 and A_e—initial and equilibrium solutions activity of ^{85}Sr, kBq cm^3, respectively, V—volume of solution, dm^3, and m—mass of a sorbent, g.

Characterization methods

Measurement of ζ-potential of the dispersed phase of manganese oxide hydrosols was performed at a laser analyzer Zetasizer Nano ZS (Malvern Instruments) at a temperature of 25 ± 0.1 °C.

XRD analysis was carried out by the diffractometer DRON-3 with Cu-K_α-monochromatizing radiation ($\lambda = 0.154184$ nm) at reflection angles 2θ from 10 to 80° to identify the phase composition of the sorbents based on manganese oxides used. The processing of diffraction data and phase identification of the samples was carried out using software "PowderX" and "WinXpow" (Version 1.04) and base of X-ray powder standards "JCPDS PDF2" (Version 1.21).

IR spectra of samples were recorded on IR spectrometer with Fourier transmittance Tenzor-27 in the range of 1800–450 cm^{-1} at room temperature, using a tableting of sorbents powder with potassium bromide.

The adsorption and textural properties of samples were estimated from isotherms of low temperature (− 196 °C) nitrogen physical adsorption–desorption via volumetric on ASAP 2020 MP surface area and porosity analyzer (Micromeritics, United States). The specific surface area was determined by the BET method (A_{BET}). The adsorption cumulative volume ($V_{BJH\ ads}$) in the range of pore from 1.7 to 300 nm, the average adsorption diameter ($D_{BJH\ ads}$), differential mesopore size distribution (dV/dlogD) calculated by Barrett-Joyner-Halendy method (BJH). Before the analysis samples were held in a vacuum for 1 h at 200 °C and a residual pressure of 133.3×10^{-3} Pa. The samples 1 and 5 were held in a vacuum for 3 h at 80 °C. The relative error in determining the pore volume was ± 1%, for the surface area and for the pore size ± 15%.

The surface morphology and element composition of manganese oxides were studied by means of the scanning electronic microscope of JSM-5610 LV with system of the chemical analysis EDX JED-2201 JEOL (Japan) with a preliminary coating of gold on the samples.

The pH of the reaction mixture and manganese oxides hydrosols was measured using the pH meter HI 221 (HANNA Instruments).

Results and discussion

Sorption properties towards strontium ions

Sorption properties of manganese oxides towards Sr^{2+} ions at the interface solid/solution substantially depend on the nature of the reducing agent and the conditions of the sorption process. So the sample prepared using H_2O_2 shows the highest sorption capacity equal to 200 mg g^{-1} in the absence of background electrolyte (Table 1). The other two manganese oxides samples obtained by reducing of $KMnO_4$ by $MnCl_2$ or PVA have lower capacitive characteristics equal to 70 and 100 mg g^{-1} respectively.

A similar dependence is observed in the introduction of 0.1 M NaCl to the model solution, when all the samples have almost a threefold decrease in sorption capacity for Sr^{2+}. When take place the sorption from solutions, including the addition of 0.05 M $CaCl_2$, a number of active sorbents based on manganese oxides significantly changes. The high sorption capacity of the sample is obtained using PVA as a reducing agent. On the background of 0.1 M NaCl and 0.05 M $CaCl_2$ this sample demonstrates almost equal to the sorption capacity, about 25–33 mg g^{-1}, while the sorbents obtained using H_2O_2 or $MnCl_2$ remove in 3–4 times lower Sr^{2+} amount from Ca^{2+} containing solutions than Na^+ containing (Table 1). This proves a higher selectivity of the manganese oxide synthesized by reducing of $KMnO_4$ by PVA compared with the other samples.

In real conditions low-active liquid radioactive waste contain trace concentrations of radionuclides ^{85,90}Sr (about 10^{-9}–10^{-13} M). It is obvious that the efficiency of sorption removal of such quantities of Sr^{2+} may differ significantly from the results obtained during the sorption of stable Sr^{2+} ions from the solutions with concentration in the range of 10^{-1}–10^{-4} M. Analysis of the data Table 1 shows that the distribution coefficient of ^{85}Sr for the obtained samples reaches a value of 3.7×10^5 cm^3 g^{-1} with sorption of ^{85}Sr from the solutions without background electrolyte. Such

Table 1 The values of sorption capacity, removal efficiency and distribution coefficient of ^{85}Sr radionuclide on manganese oxides (V/m = 250, pH 5.7 ± 0.2)

Reducing agent	Background solution	Sorption capacity (A), mg g^{-1}	Distribution coefficient (K_d) × 10^{-3}, cm^3 g^{-1}
$MnCl_2$	H_2O	70	21.1
	0.1 M NaCl	22	0.12
	0.05 M $CaCl_2$	8	0.87
H_2O_2	H_2O	200	367
	0.1 M NaCl	78	47.4
	0.05 M $CaCl_2$	15	0.15
PVA	H_2O	100	18.1
	0.1 M NaCl	25	48.6
	0.05 M $CaCl_2$	33	0.14

high sorption characteristics of sorbents are quite expected due to absence of the competing ions. The introduction of 0.1 M NaCl is accompanied by a tenfold decrease in the K_d values for ^{85}Sr. The best selective properties (K_d ^{85}Sr = 870 cm^3 g^{-1}) on the background of 0.05 M $CaCl_2$ shows a sample obtained using $MnCl_2$. The established differences of the sorption-selective properties of manganese oxides in experiments with stable ions of Sr^{2+} and radionuclide ^{85}Sr can be interpreted when studying the mechanism of sorption.

XRD analysis

Phase and chemical composition are the main factors that influence on the selective properties of manganese oxides towards Sr^{2+} ions. The initial sorbents obtained using inorganic reducing agents have low crystallinity and consist mainly $K_{1.33}Mn_8O_{16}$ (96–151–8323—number of phase in COD ("Crystallography Open Database") and β-MnO_2 (96–151–4102) oxides with a layered structure (check Fig. 1a, c). After sorption of Sr^{2+} in the samples is ongoing structuring and the Sr-containing phase $Sr_{0.72}Mn_8O_{16}$ (41–314) is appeared on the X-ray diffractogrammes (Fig. 1b, d). The sorbent obtained by using PVA consists a well-crystallized oxides $K_{1.33}Mn_8O_{16}$ (96–151–8323) and MnO (96–900–6665) with a mixture of K_2CO_3 (96–210–7220) (soluble in water—110.5 g in 100 g H_2O at 25 °C) and KOH (96–153–4406) (Fig. 1e). The formation of the hydroxide occurs in the interaction of $KMnO_4$ with PVA is mainly at the stage of sol obtaining, which completely fails to wash from the hydrogel of the manganese oxide. Further, the high temperature processing of manganese oxide, during thermo-oxidative degradation of PVA oxidation products, is formed K_2CO_3. For a sorbent obtained using PVA were detected other Sr-containing phase—$SrMnO_3$ (96–152–9599), $SrCO_3$ (96–901–3803) (soluble in water—2×10^{-3} g in 100 g H_2O at 25 °C) and SrO (96–110–1041) in contrast with sorbents synthesized with inorganic reducing agents (Fig. 1f).

Thus, if in the case of manganese oxides obtained using inorganic reducing agents we can talk about a predominantly ion-exchange sorption of strontium ions, the sorption mechanism for the sample on the basis of PVA involves mainly chemical interaction with K_2CO_3 and to a less degree of ion-exchange.

FT-IR analysis

IR spectra of manganese oxides recorded at the 1800–450 cm^{-1} before and after sorption of Sr^{2+} ions allow more detailed study of the sorption mechanism and to identify the differences between the samples (Fig. 2). For all samples after sorption, the intensity of absorption band around 1620 cm^{-1} which is characteristic for stretching vibrations of O–H groups associated with the manganese atoms of the crystal lattice are raised, indicating the course of hydration process. For the sample synthesized using the H_2O_2, the intensity of the absorption bands at 613 and 473 cm^{-1} related to the stretching vibrations of Mn–O characteristic of well-crystallized mixtures of phases (β-MnO_2 + γ-MnO_2) are significantly increases after sorption of Sr^{2+} ions. In the case of the reducing agent $MnCl_2$ for initial samples and manganese oxides after sorption a clear band of about 655, 610, 530 and 475 cm^{-1} which are characteristic of valence fluctuations when the Mn–O in the structure of β-MnO_2 are observed. Intense bands at 615 and 480 cm^{-1} inherent to the stretching vibrations of Mn–O phase in $SrMnO_3$ appear in the sample obtained using the PVA after the sorption of Sr^{2+} ions. At the same time absorption band with low intensity in the area of 1080 cm^{-1} corresponding to the stretching vibrations of when the Mn^{3+}–O suggests the partial substitution of

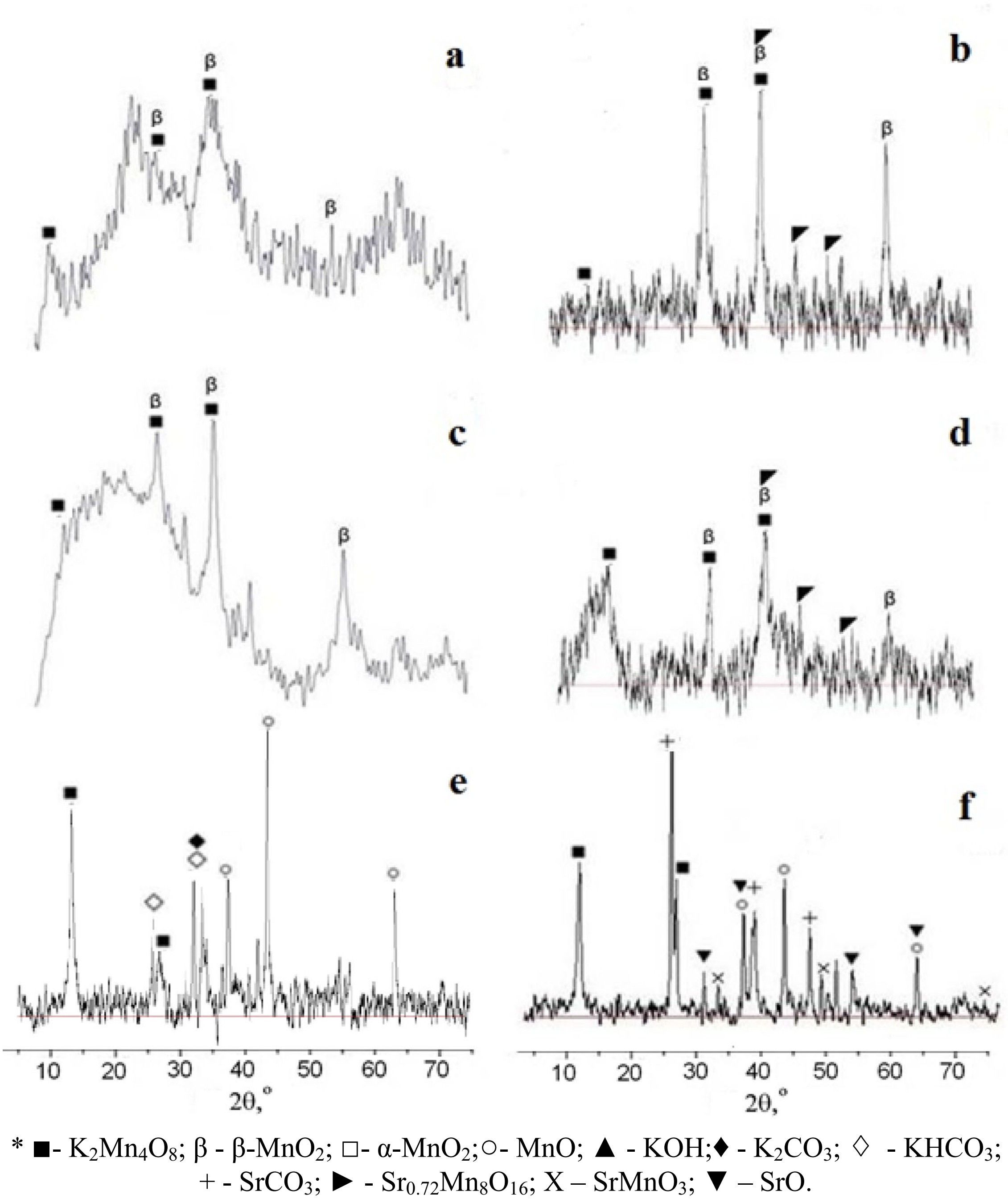

Fig. 1 XRD patterns of the manganese oxide samples synthesized by reduction of $KMnO_4$ by H_2O_2 (**a**, **b**), $MnCl_2$ (**c**, **d**), and PVA (**e**, **f**) before (**a**, **c**, **e**) and after (**b**, **d**, **f**) sorption of strontium ions

Mn^{4+}–Mn^{3+} ions. The absorption band in the region of 770–750 cm^{-1} is characteristic of manganese oxides with tunnel structure and it is present in the IR-spectra of all samples [30].

N_2 adsorption–desorption study

Nitrogen adsorption results indicate essentially distinctions in characteristic signs and features of the measured isotherms, in hysteresis behavior of adsorptive, in the values of pore volume and surface area of manganese oxide porous solids obtained with different reducers (Fig. 3, Table 2). The nitrogen sorption isotherms on manganese

Fig. 2 IR spectra of the manganese oxide samples synthesized by reduction of $KMnO_4$ by H_2O_2 (**a**), $MnCl_2$ (**b**) and PVA (**c**)

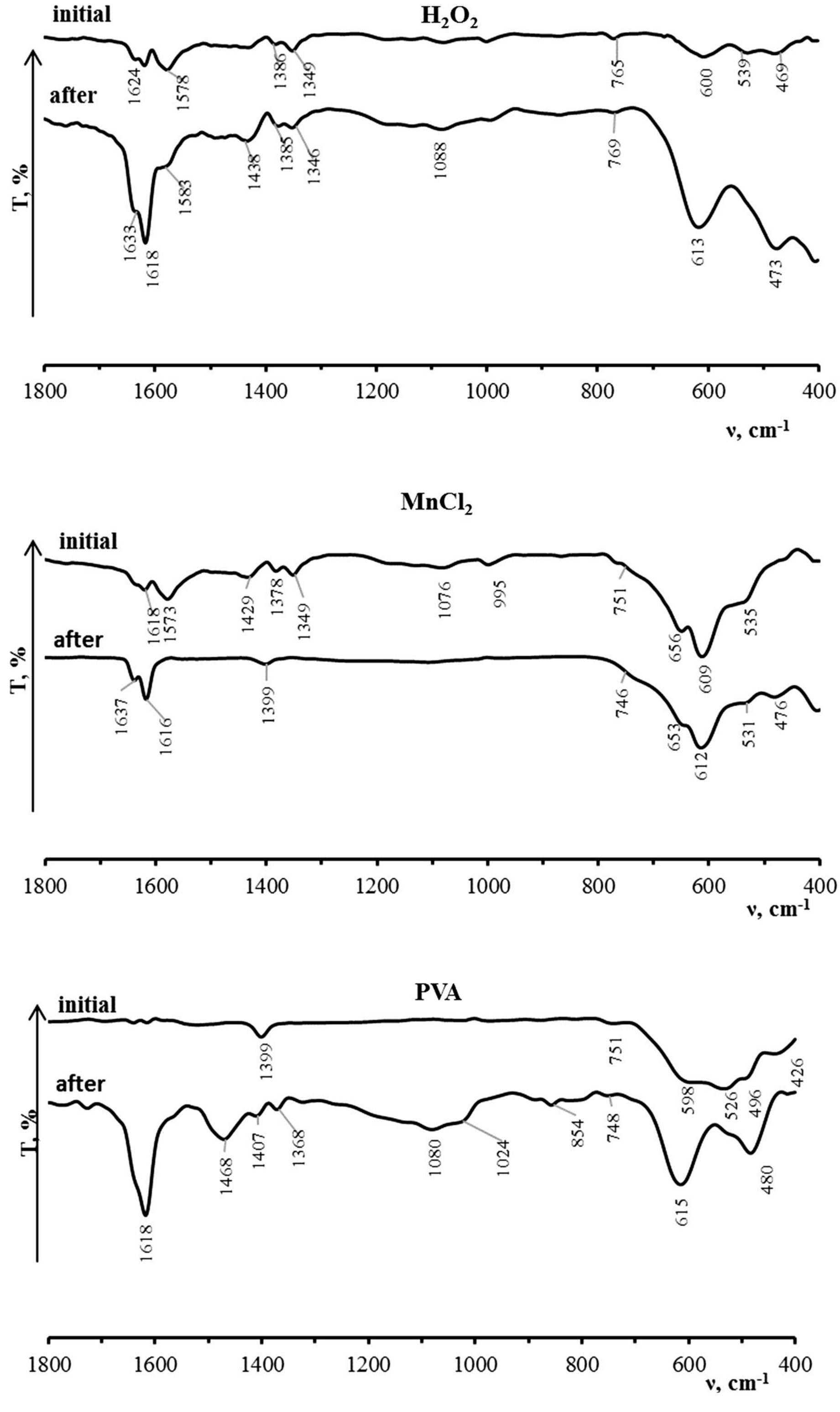

oxide obtained with hydrogen peroxide belong, on IUPAC classification, to the Type IV isotherm given by many mesoporous adsorbents. Isotherms of this type have the same overall shape as a normal Type II isotherm, obtained with non-porous or macroporous adsorbents, up to the value of relative pressure p/p_0 at which the capillary condensation begins resulting in the hysteresis loop and adsorption growth. The hybrid Type (H1+H2) hysteresis loop given by "peroxide" sample before sorption of Sr^{2+} ions correlates with texture of adsorbent. The Type H1 loop

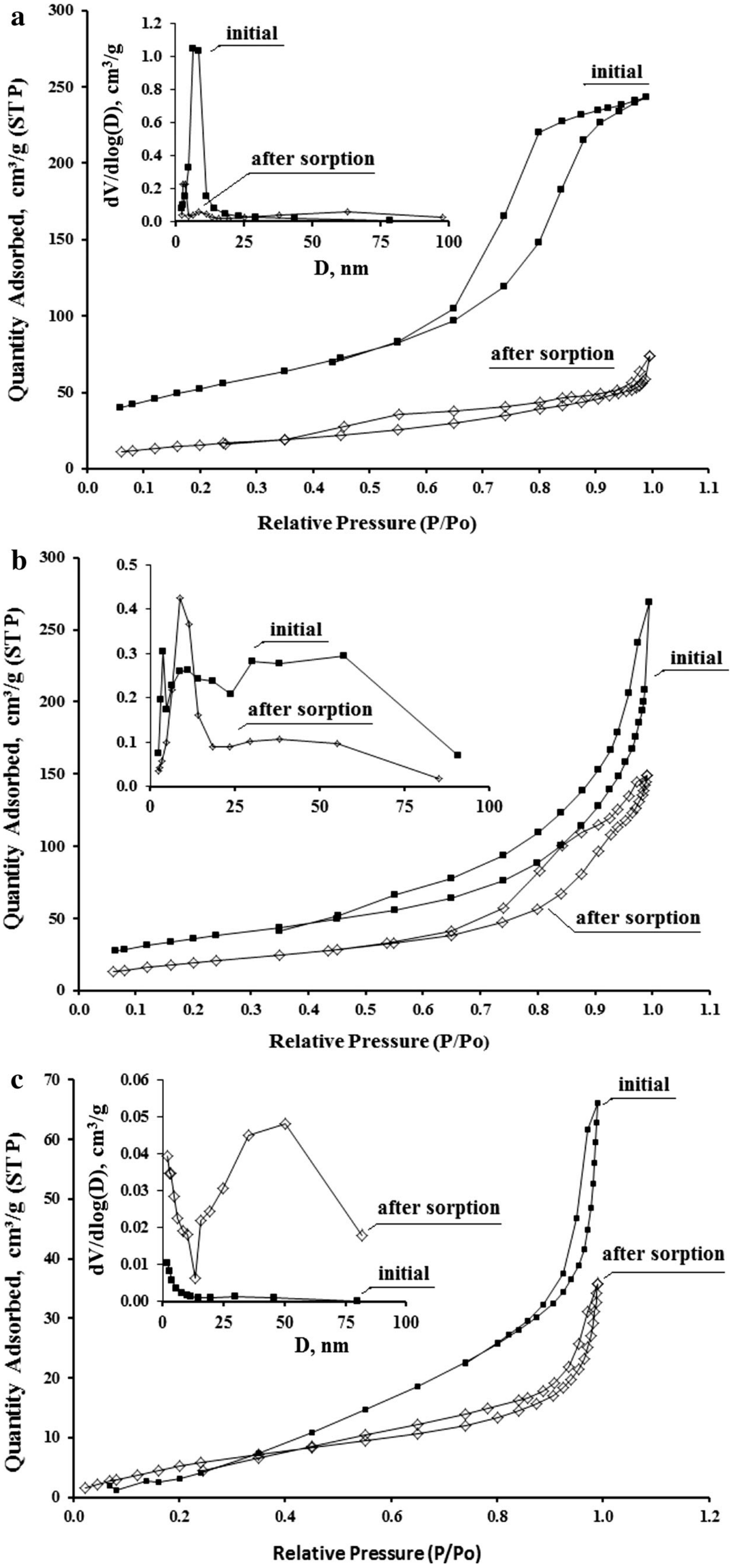

Fig. 3 Isotherms of nitrogen adsorption–desorption calculated from pore size distribution of xerogels of manganese oxide synthesized by reduction of $KMnO_4$ by H_2O_2 (**a**), $MnCl_2$ (**b**), and PVA (**c**), before and after sorption of strontium ions

Table 2 The adsorptive properties of manganese oxides before and after sorption of Sr ions

Reducing agent	Sorption of Sr^{2+}	A_{BET}, $m^2\ g^{-1}$	V_{BJHdes}, $cm^3\ g^{-1}$	D_{BJHdes}, nm
$MnCl_2$	Before	212	0.260	4.7
	After	72	0.233	9.3
H_2O_2	Before	189	0.384	6.6
	After	58	0.118	6.1
PVA	Before	11	0.102	8.3
	After	24	0.056	7.8

is associated with narrow pore size distribution of fairly uniform “cylindrical” mesopores (Fig. 3a). The Type H2 loop indicates more complex porous structure in which the effects of percolation and pore blocking are shown. Nitrogen sorption isotherms for two other samples received with $MnCl_2$ and/or PVA don’t exhibit any limiting adsorption at high p/p_0 values and can be carried to pseudo-type II isotherm. Such not completely reversible isotherms, according to Kenneth S.W. Sing, are associated with adsorbents containing slit-shape pores and consisting of friable aggregates of platy particles. Their adsorption curve entirely repeats the path of the Type II adsorption isotherm, but desorption branch follows on other way, leading to the hysteresis limited by area of multilayer adsorption.

Sorption of Sr^{2+} significantly influences the adsorption and capillary-condensation properties of manganese oxides. So this circumstance considerably affects the properties of xerogel obtained with H_2O_2. The specific characteristics of surface area and pore volume decrease by 3.3 times after sorption of Sr^{2+} ions. When using $MnCl_2$ the surface area decreases by 2.9 times after sorption of Sr^{2+}, and in case of PVA the surface area is equal only to 11–24 $m^2\ g^{-1}$ and remains poorly developed after sorption of Sr^{2+} ions. Isotherms of pseudo-type II don’t provide reliable assessment neither specific pore volume, nor pore size distribution. But in the samples received with $MnCl_2$ or with PVA it is possible to record after sorption of Sr^{2+}, first, the decrease in pore volume proportionally to falling surface area, therefore the pore size remains almost invariable (Table 2), and, secondly, the full modification of pore size distribution (Fig. 3b, c). It is undoubted that the displaying Sr^{2+} sorption in case of the samples obtained with H_2O_2 and in case of the sample obtained with H_2O_2 differ one from another. So inclusion of Sr^{2+} ions into the “peroxide” sample facilitates diffusion of nitrogen molecules in mesopores, and the mean mesopore diameter increases (Table 2). At the same time the pore size distribution of cylindrical mesopores remains uniform after sorption of Sr^{2+} ions, but pore volume falls (Fig. 3a).

Thus, it should be noted that the growth of the mean mesopore diameter of the “peroxide” sample observed after Sr^{2+} sorption is obliged to fast loss of surface area in combination with homogeneous “volume shrinkage” of manganese oxide xerogel. Most likely, the positive Sr^{2+} ions sorbed by ion-exchange with the cations compensating a charge of manganese oxide framework are rather evenly dispersed all over the volume of crystals what SEM–EDX analysis data confirm.

SEM–EDX analysis

The results of SEM–EDX analyses prove that in the case of the manganese oxide obtained by reduction of $KMnO_4$ by H_2O_2, Sr^{2+} is distributed uniformly across the surface of the sorbent with the presence of small areas with higher content of Sr^{2+} component. On the sample obtained with $MnCl_2$ Sr^{2+} is appeared very weak which indicates about it low content. The highest Sr^{2+} content determined on the surface of the sorbent is detected in the sample obtained using PVA. In the pictures clearly seen as Sr^{2+} concentrates on separate sites of manganese oxide surface in the form of individual phases. Combined with the XRD data we can assume that it is the particles of $SrCO_3$ (Fig. 4).

According to the element analysis of the manganese oxides before and after sorption of Sr^{2+} ions, in all samples observed the expected decrease in the K^+ content and identification of Sr^{2+} in the range of 1.0 at.%. It was revealed that the number of Sr^{2+} ions in the sample, synthesized using PVA significantly greater than that of manganese oxides obtained with inorganic reducing agents. These results are in a good agreement with the ion-exchange or chemisorption mechanism of strontium uptake onto manganese oxides obtained using either inorganic reducing agent (H_2O_2, $MnCl_2$), or PVA respectively (Table 3).

Conclusions

The manganese oxides sorbents of Sr^{2+} ions were synthesized by sol–gel method reducing of $KMnO_4$ by different reagents—H_2O_2, $MnCl_2$ and PVA. Their sorption characteristics towards stable (Sr^{2+}) and radioactive (^{85}Sr) ions were established. The sorbent obtained using H_2O_2 as a reducing agent has highest sorption properties (sorption capacity 200 mg g^{-1} and K_d ^{85}Sr 3.67×10^5 $cm^3\ g^{-1}$).

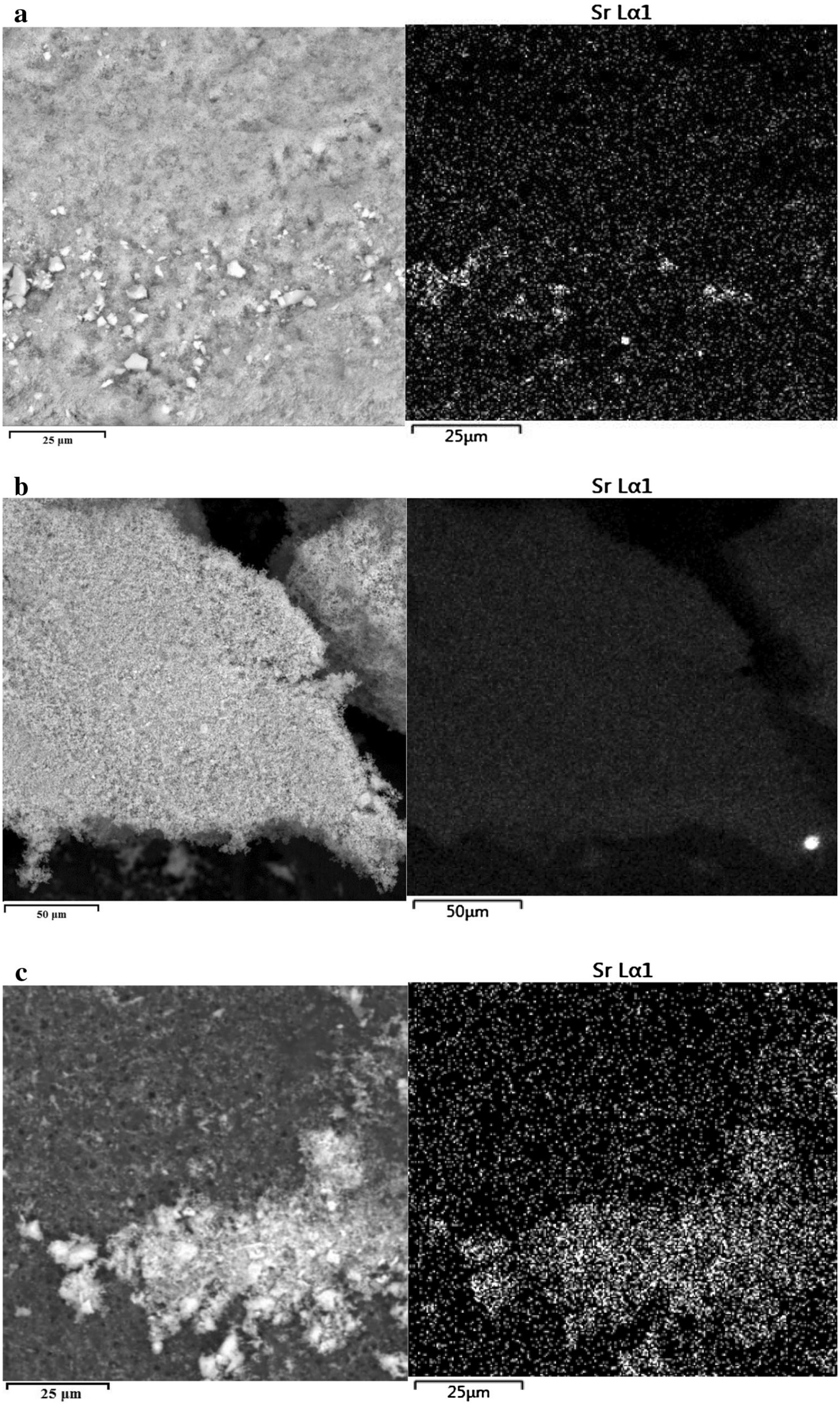

Fig. 4 SEM photo of the manganese oxide samples synthesized by reduction of $KMnO_4$ by H_2O_2 (**a**), $MnCl_2$ (**b**), and PVA (**c**) with the mapping of Sr distribution (white colour)

Table 3 Element composition of manganese oxides before and after sorption of Sr ions

Reducing agent	Sorption of Sr^{2+}	Element composition, at.%			
		O	Mn	K	Sr
$MnCl_2$	Before*	38.8	59.7	0.8	–
	After	63.0	36.54	0.25	0.21
H_2O_2	Before	24.8	73.7	1.5	–
	After	54.36	45.4	0.1	0.14
PVA	Before**	13.3	70.7	11.2	–
	After	60.3	33.7	4.9	1.1

*0.7 at. % refers to hydrogen (H) **4.8 at. % refers to carbon (C)

Manganese oxide obtained using H_2O_2 provides the most selective removal of Sr^{2+} ions in presence of 0.1 M NaCl (sorption capacity 78 mg g^{-1} and K_d ^{85}Sr 4.74×10^4 cm^3 g^{-1}). In presence of 0.05 M $CaCl_2$ sorbent synthesized using PVA has the highest sorption capacity—33 mg g^{-1} and the sample obtained using $MnCl_2$ has the highest K_d ^{85}Sr—8.70×10^2 cm^3 g^{-1}.

On the basis of XRD, FT-IR, N_2 adsorption–desorption and SEM–EDX data was proposed a possible mechanism of Sr^{2+} ion uptake by manganese oxides. In case of manganese oxides obtained with inorganic reducing agents (H_2O_2 and $MnCl_2$) Sr^{2+} ions are removed dominantly by ion-exchange mechanism. For samples, obtained using PVA a chemisorption mechanism was proposed. It has been confirmed with the formation of $SrMnO_3$ and $SrCO_3$ while ion-exchange mechanism—with the replacement of K^+ and Mn^{2+} ions in $K_{1.33}Mn_8O_{16}$ on Sr^{2+}. It was shown that obtained sorbents are promising for liquid radioactive water treatment from Sr radionuclides.

Acknowledgements This work was financially supported by the State Program of Scientific Research (grant# 1.05).

References

1. Fonollosa E, Nieto A, Penalver A, Aguilar C, Borrull F (2015) Presence of radionuclides in sludge from conventional drinking water treatment plants. J Environ Radioact 141:24–31
2. Rana D, Matsuura T, Kassim MA, Ismail AF (2013) Radioactive decontamination of water by membrane processes—a review. Desalination 321:77–92
3. Laraia M (2015) Radioactive contamination and other environmental impacts of waste from nuclear and conventional power plants, medical and other industrial sources. In: van Velzen L (ed) Environmental remediation and restoration of contaminated nuclear and norm sites. Woodhead Publishing, Cambridge, pp 35–56
4. Panchenko SV, Linge II, Vorobyeva LM, Melikhova EM, Utkin SS, Kryshev II, Sazykina TG, Geraskin SA (2015) Radio-ecological situation in the regions of location of Rosatom enterprises. SAM polygraphist, Moscow
5. Lavrentyeva GV (2014) Characteristic of pollution with groundwater inflow ^{90}Sr natural waters and terrestrial ecosystems near a radioactive waste storage. J Environ Radioact 135:128–134
6. Yavari R, Huang YD, Mostofizadeh A (2010) Sorption of strontium ions from aqueous solutions by oxidized multiwall carbon nanotubes. J Radioanal Nucl Chem 285:703–710
7. Zhang L, Wei J, Zhao X, Li F, Jiang F, Zhang M, Cheng X (2016) Competitive adsorption of strontium and cobalt onto tin antimonate. Chem Eng J 285:679–689
8. Rabideau AJ, Benschoten JV, Patel A, Bandilla K (2005) Performance assessment of a zeolite treatment wall for removing ^{90}Sr from groundwater. J Contam Hydrol 79:1–24
9. Pshinko GN, Puzyrnaya LN, Shunkov VS, Kosorukov AA, Demchenko VY (2016) Removal of cesium and strontium radionuclides from aqueous media by sorption onto magnetic potassium zinc hexacyanoferrate(II). Radiochemistry 58:491–497
10. Kulyukhin SA, Krasavina EP, Rumer IA, Mizina LV, Konovalova NA, Gredina IV (2011) Effect of complexing anions on sorption of U(VI), ^{90}Sr, and ^{90}Y from aqueous solutions on layered double hydroxides of Mg, Al, and Nd. Radiochemistry 53:504–509
11. Li Q, Liu HN, Liu TY, Guo M, Qing BJ, Wu ZJ (2010) Strontium and calcium ion adsorption by molecularly imprinted hybrid gel. Chem Eng J 157:401–407
12. Özeroğlu C, Bilgiç ÖD (2015) Use of the crosslinked copolymer functionalized with acrylic acid for removal strontium ions from aqueous solutions. J Radioanal Nucl Chem 305:551–565
13. Özeroğlu C, Keçeli G (2006) Removal of strontium ions by a crosslinked copolymer containing methacrylic acid functional groups. J Radioanal Nucl Chem 268(2):211–219
14. Milyutin VV, Ryabchikov BE (2015) Hydrometallurgical methods of treatment of radioactive waste and natural waters: educational materials. Dmitry Mendeleev University of Chemical Technology of Russia, Moscow
15. Villard A, Siboulet B, Toquer G, Merceille A, Grandjean A, Dufrêche JF (2015) Strontium selectivity in sodium nonatitanate $Na_4Ti_9O_{20}{\cdot}xH_2O$. J Hazard Mater 283:432–438
16. Zhang L, Wei J, Zhao X, Li F, Jiang F, Zhang M, Cheng X (2016) Removal of strontium(II) and cobalt(II) from acidic solution by manganese antimonate. Chem Eng J 302:733–743
17. Todorovic M, Milonjic SK, Gal IJ, Como JJ (1991) Kinetics of sorption of some long-lived fission products on inorganic sorbents. In: Proceedings of a final research coordination meeting held in Rez, Czechoslovakia, pp 31–46
18. Wang LM, Chen J, Ewing RC (2004) Radiation and thermal effects on porous and layer structured materials as getters of radionuclides. Curr Opin Solid State Mater Sci 8:405–418
19. Axe L, Tyson T, Trivedi P, Morrison T (2000) Local structure analysis of strontium sorption to hydrous manganese oxide. J Colloid Interface Sci 224:408–416
20. Marsh SF, Pillay KKS (1993) Effects of ionizing radiation on modern ion exchange materials. Los Alamos National Laboratory, Los Alamos, pp 1–15
21. Hashemzadeh F, Motlagh MMK, Maghsoudipour A (2009) A comparative study of hydrothermal and sol–gel methods in the synthesis of MnO_2 nanostructures. J Sol-Gel Sci Technol 51:69–174
22. Kumagai N, Komaba S, Sakai H, Kumagai N (2001) Preparation of todorokite-type manganese-based oxide and its application as lithium and magnesium rechargeable battery cathode. J Power Sources 97–98:515–517
23. Pakarinen J, Koivula R, Laatikainen M, Laatikainen K, Paatero E, Harjula R (2010) Nanoporous manganese oxides as environmental protective materials—effect of Ca and Mg on metals sorption. J Hazard Mater 180:234–240

24. Jonghyuk L, Ju JB, Cho WI, Cho BW, Oh SH (2013) Todorokite-type MnO_2 as a zinc-ion intercalating material. Electrochim Acta 112:138–143
25. Milyutin VV, Nekrasova NA, Kozlitin EA (2015) Removal of radionuclides and corrosion products from neutral and weakly alkaline solutions by microfiltration. In: Proceedings of the Kola Science Center of the Russian Academy of Sciences, Moscow, pp 418–421
26. Dyer A, Pillinger M, Newton J, Harjula R, Moller T, Amin S (2000) Sorption behavior of radionuclides on crystalline synthetic tunnel manganese oxides. J Chem Mater 12:3798–3804
27. Denton M, Manos M, Kanatzidis M (2009) Highly selective removal of cesium and strontium. In: Materials of waste management symposium, Phoenix, pp 1593–1601
28. Ivanets AI, Kuznetsova TF, Prozorovich VG (2015) Sol-gel synthesis and adsorption properties of mesoporous manganese oxide. Rus J Phys Chem A 89:481–486
29. Ivanets AI, Prozorovich VG, Krivoshapkina EF, Kuznetsova TF, Krivoshapkin PV, Katsoshvili LL (2017) Physicochemical properties of manganese oxides obtained via the sol–gel method: the reduction of potassium permanganate by polyvinyl alcohol. Rus J Phys Chem A 91:1486–1492
30. Kang L, Zhang M, Liu Z-H, Ooi K (2007) IR spectra of manganese oxides with either layered or tunnel structures. Spectrochim Acta Part A 67:864–869